



MADRID
inter.noise 2019
June 16 - 19

NOISE CONTROL FOR A BETTER ENVIRONMENT

Numerical prediction of aerodynamic noise radiated from a propeller of unmanned aerial vehicles

Lee, Hakjin¹

Lee, Duck-Joo²

Korea Advanced Institute of Science and Technology (KAIST)

KAIST, 291 Daehak-ro, Yuseong-gu, Daejeon 34141, Republic of Korea

ABSTRACT

The demand for the development of small unmanned aerial vehicles (UAVs) has been growing in a wide range of industrial and commercial applications. UAV based on the multi-rotor platform, commonly called as a drone, has received considerable attention, owing to a user-friendly control system, simple mechanical structure, and vertical take-off and landing (VTOL) ability. However, the noise problem is one of the major hindrances for the widespread use of a drone, since the sound pressure level associated with the drone could lead to severe problems in mental health, such as annoyance, psychological distress, and stress. The main objective of this work is to predict the aerodynamic noise from quadcopter UAV, and the sound pressure level of the quadcopter is compared with that of isolated rotor one to investigate rotor-to-rotor interaction effects in terms of noise characteristics. In this study, nonlinear vortex lattice method (NVLM) coupled with vortex particle method (VPM) and acoustic analogy based on Farassat-1A formula are adopted as aeroacoustic analysis model, and numerical predictions are validated against measurements. Noise predictions of quadcopter configurations with different separation distances in hover flight are conducted. Discussion in this work will help to achieve a better understanding of the noise characteristics of multi-rotor systems.

Keywords: Unmanned Aerial Vehicles (UAVs), Quadcopter, Rotor-to-rotor interaction. Noise, Environment, Annoyance

I-INCE Classification of Subject Number: 76

1. INTRODUCTION

Recently, a small size of unmanned aerial vehicles (UAVs) based on the multi-rotor platform, commonly referred to as drones, have received considerable attention, owing to a user-friendly control system, easy accessibility, simple mechanical structure, and vertical take-off and landing (VTOL) ability. Drone-related industry has continued to grow worldwide. However, social and environmental problems related to noise pollution have been also increased because the sound pressure level radiated from the drones could exceed the background noise that can have a significant impact on the people. Hence, drone noise could lead to severe problems in mental health, such as annoyance, anxiety, and stress. One of the reasons for this annoyance is that drone noise is emitted

¹ hakjin@kaist.ac.kr

² djlee@kaist.edu

periodically with a broad range of frequencies. It is reported that drone noise is more annoying than equally loud sources such as airport and traffic noise. Therefore, several countries have established a special regulation for drone noise to limit the sound pressure level. For mitigating the noise pollution problems, the drone should be designed not only to be aerodynamically efficient but also to be quiet. Thus, reducing the noise of drone is becoming more and more important. An assessment of drone noise should be included early in the design process rather than a problem to be corrected during the production or testing stages.

In the case of the small UAVs, the multi-rotor systems, such as quadcopter or octocopter, are preferable to swashplate mechanism because they can easily generate the required aerodynamic performance and stabilize vehicle's attitude using a simple flight control algorithm. Compared to the rotary vehicles with a single main rotor, the rotor-to-rotor interaction severely occurs in multi-rotor configuration. Rotor interactional effects cause highly complex wake structures and unsteady wake flow behavior around the vehicles, thus leading to significant thrust fluctuation and a rise in the level of tonal and broadband noise. Therefore, mutual rotors interaction should be investigated to mitigate drone noise pollution.

The main aim of this research is to simulate the wake flow of quadcopter UAV and study its impacts on aeroacoustics characteristics. In this work, nonlinear vortex lattice method (NVLM) with vortex particle method (VPM) and acoustic analogy based on Farassat-1A formulation were adopted as the aerodynamic and aeroacoustic models, respectively. Prediction of isolated rotor configuration was compared against available measurements to validate the prediction methods. Calculations for the quadcopter UAV showed that noise level significantly increased due to unsteady aerodynamic loads caused by the rotor interactional effects.

2. NUMERICAL METHOD

2.1 Model description

Numerical simulation of the DJI Phantom 2 model was carried out to predict the aerodynamic noise emitted from multi-copter UAVs, and investigate the effects of the mutual rotor-to-rotor interaction on the aeroacoustic performance. DJI Phantom 2 is the second generation of Phantom RC quadcopters developed from DJI corporation, and it is one of the most popular commercial UAVs. It is a quadcopter with four connecting arms and fuselage as depicted in Figure 1. Two-bladed DJI 9443 propeller with a diameter of 0.24 m (9.45 in.) are mounted on the end of the connecting arms and a diagonal length between rotors is 0.35 m. Two sets of rotors are designed to rotate in the opposite direction to balance the angular momentum and maintain the rotational attitude of quadcopter; two of rotors rotate in a clockwise direction, the others rotate in a counter-clockwise direction. The blade pitch angle is fixed, hence the attitude of the quadcopter is controlled by adjusting the rotational speed of each rotor that is directly connected to the electrically driven motor. In this work, the rotor speed was changed from 3,000 to 7,200 rpm, which are corresponding to incompressible and low Reynolds number flow as listed in Table 1.

Hover performance in terms of the thrust force and noise level of isolated DJI 9443 rotor blade was measured for a wide range of rotation rates at structural acoustic loads and transmission (SALT) facility in NASA Langley Research Center as shown in Figure 2. Isolated DJI 9443 propeller has directly mounted the electrically driven motor. Thrust force, acoustic pressure, and rotation rate of the propeller are measured by a single-axis load cell, 1/4" Type 4939 free-field Brüel & Kjaer microphones and a laser sensor tachometer, respectively. A total of five microphones in arc array configuration with an

incremental angle of 22.5° degrees are positioned, from 45° below the rotating plane to 45° above the rotating plane as depicted in Figure 2. A radial distance between the motor hub and microphones is 1.907 m corresponding to approximately $16R$. Here R is the rotor radius. The experimental data were used to validate the accuracy of present numerical methods.



Figure 1. DJI Phantom 2 configuration

Table 1. Detailed descriptions of DJI Phantom 2 model

Properties	Values
Propeller	DJI 9443 model
Number of rotors	4
Number of blades	2
Rotor diameter, D	0.24 m
Diagonal length, L	0.35 m
Rotating speed, Ω	3,000 ~ 7,200 rpm
Tip Mach number, M_{tip}	0.1 ~ 0.26
Reynolds number, Re_c	3,000 ~ 70,000

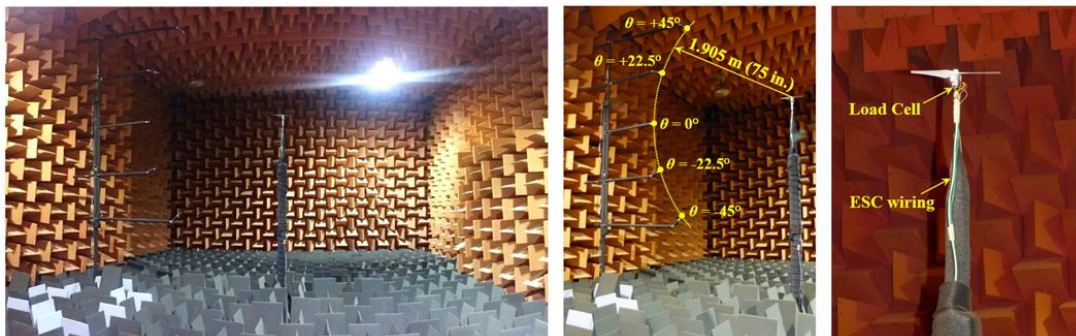


Figure 2. Anechoic chamber facility and microphone array with rotor-motor apparatus¹

2.2 Aerodynamic model

To assess the aerodynamic noise radiated from the rotor blades, the aerodynamic loads on the rotor blades should be evaluated. Reynolds number plays a critical role in determining aerodynamic characteristics of the airfoil. When the airfoil encounters the low Reynolds number flow, a slope of lift curve is no longer 2π and lift coefficient tends to nonlinearly change with respect to the angle of attack. Therefore, these nonlinear aerodynamic characteristics should be considered to accurately predict the aerodynamic performance of a small size of UAVs, which mostly operate in the low Reynolds number range from 10^4 to 10^5 . (Helicopters generally operate over the Reynolds number of 10^6 .)

Vortex lattice method (VLM) is one of the most practical approaches for the comprehensive analysis of the rotary systems, such as propeller, helicopter and wind turbine blades. It is capable of calculating the aerodynamic loads on the rotor blades with affordable computational costs. However, VLM is intrinsically impossible to consider the nonlinear variation in lift curve slope because it was derived based on an assumption of the incompressible and potential flows. In this work, the nonlinear vortex lattice method (NVLM) is adopted as the aerodynamic model to simulate the flow field around single- or multi-rotor configurations and calculate the primary variables for aeroacoustic analysis. NVLM includes the airfoil look-up table and iterative vortex strength correction to overcome the limitation of existing VLM as mentioned above, it has a great ability to consider the nonlinear aerodynamic characteristics mainly introduced by the low Reynolds number flow²⁻⁴. The aerodynamic loads on the rotor blades will be evaluated using the sectional lift and drag coefficients obtained from airfoil look-up table as a function of local inflow velocity and effective angle of attack, which are computed based on the potential solutions. The strength of vortex ring elements distributed on the rotor blades (bound vortex) is corrected by matching the relations between thin airfoil theory and Kutta-Joukowski theory. In addition, the strength of the nascent wake elements which are recently shed from the trailing edges was already determined at the previous time step by imposing Kutta condition. Therefore, an influence of low Reynolds number flow on the wake vortex strength and wake structures can be also taken into account.

For the numerical simulation, the rotor blade of UAV is modeled by distributing quadrilateral vortex ring elements on the camber surface in the chordwise and spanwise directions as depicted in Figure 3. The surface grid resolution is 25 (chordwise) \times 40 (spanwise). The blades rotate 5 degrees per time step to obtain better flow and acoustic solutions, and the total number of revolution is 20 including 1 revolution for slow starting to prevent wake instability problem.

2.2 Rotor wake model

NVLM is tightly integrated with vortex particle method (VPM) for modeling the rotor wake. The rotor wake shed from a full span of the rotor blades were represented as vortex particles, rather than vortex filaments, as shown in Figure 3. The vortex particles mutually influence each other and are allowed to freely distort and move to the downstream. Time integration algorithm is required to conduct time-accurate simulation and to update the convection velocity and location of vortex particles. 2nd-order Runge-Kutta method is used here. The convection velocity is the sum of the free stream velocity, the self-induced velocity due to the bound vortices, and the wake-induced velocity due to wake vortices. The velocity induced by the wake particles is calculated using the Biot-Savart law with a high-order algebraic smoothing function.

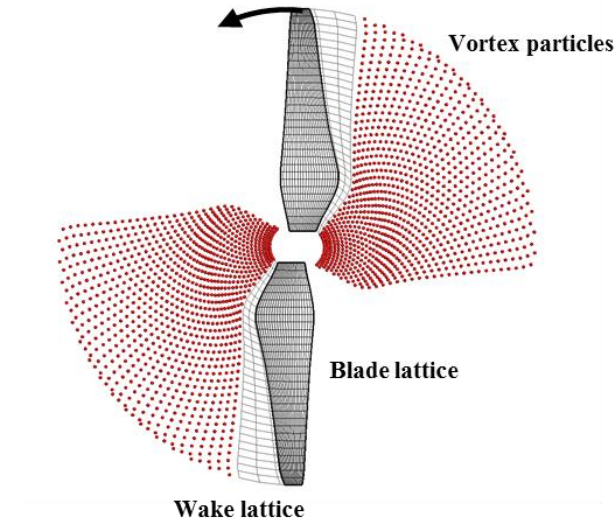


Figure 3. Rotor blade and wake modeling

2.2 Aeroacoustic model

Major sources of the rotor noise can be generally classified into non-deterministic and deterministic components; The former contains turbulence ingestion noise, blade-wake interaction noise, airfoil-self noise, while the latter includes thickness noise, loading noise, blade vortex interaction (BVI) noise, and high-speed impulsive (HSI) noise. The interaction of atmospheric turbulence with the boundary layer on the rotor blade leads to the unsteady pressure fluctuation that causes the radiation of turbulence ingestion noise. Blade-wake interaction noise is produced from mutual interaction between rotating blades and rotor wake. The radiation of airfoil self-noise can be typically divided into five mechanisms that were associated with the specific laminar or turbulent boundary-layer phenomena on the blade surfaces. Thickness and loading noise are mainly associated with rotating blades, and they have the periodic and tonal noise characteristics, thus leading to high sound pressure level at the rotor blade passage frequency (BPF) and harmonics. Thickness noise occurs due to the flow disturbance excited by the movement of the rotor blades and loading noise is generated from the pressure fluctuation caused by the aerodynamic loads acting on the surface of the rotor blades.

In this work, predicting the deterministic noise components including thickness and loading noise of isolated rotor and quadcopter configurations are primarily discussed. BVI and HSI noise are not directly related to the aerodynamic noise of small size UAV propeller because BVI noise is typically the most intense source of noise when the rotary wing vehicles operate in descending flight with low-speed and HSI noise is mainly associated with transonic flow and shock phenomena that can occur the advancing side of the helicopter rotor disk. The sound pressure levels of the thickness and loading noise are evaluated through an acoustic analogy using Farassat 1A formulation that is a solution for an arbitrary moving surface of the Ffowcs Williams-Hawkings (FW-H) equation with neglecting the quadrupole source term⁵. The thickness and loading noise are modeled using surface sources in terms of monopole and dipole as in Equations 1-3.

$$p'(\mathbf{x}, t) = p'_T(\mathbf{x}, t) + p'_L(\mathbf{x}, t) \quad \text{Eq. (1)}$$

$$p'_T(\mathbf{x}, t) = \frac{1}{4\pi} \int_{f=0} \left[\frac{\rho_0 (\dot{v}_n + v_{\dot{n}})}{r |1 - M_r|^2} \right]_{ret} dS + \frac{1}{4\pi} \int_{f=0} \left[\frac{\rho_0 v_n (r \dot{M}_r + a_0 M_r - a_0 M^2)}{r^2 |1 - M_r|^3} \right]_{ret} dS \quad \text{Eq. (2)}$$

$$p'_L(\mathbf{x}, t) = \frac{1}{4\pi a_0} \int_{f=0} \left[\frac{\dot{l}_r}{r |1 - M_r|^2} \right]_{ret} dS + \frac{1}{4\pi} \int_{f=0} \left[\frac{l_r - l_M}{r^2 |1 - M_r|^2} \right]_{ret} dS + \frac{1}{4\pi a_0} \int_{f=0} \left[\frac{l_r (r \dot{M}_r + a_0 M_r - a_0 M^2)}{r^2 |1 - M_r|^3} \right]_{ret} dS \quad \text{Eq. (3)}$$

Here $p'_T(\mathbf{x}, t)$ and $p'_L(\mathbf{x}, t)$ denote the acoustic pressure due to thickness and loading, respectively. l_r is the component in the radiation direction of the local force that acts on the fluid due to the surface, v_n is the local velocity of the blade surface in the direction normal to the blade surface, M_r is the component of velocity in the radiation direction normalized by the speed of sound in quiescent medium a_0 , and the dot over a symbol stands for the time-derivative terms with respect to the source-time.

3. RESULTS

3.1 Isolated rotor configuration

In this work, only the isolated rotor and four rotors were considered without connecting arms and fuselage configuration. Rotor planform geometry in terms of chord and twist angle distributions can be obtained from the reference¹, and sectional profiles of the rotor blades are extracted using digital image processing technique. As aforementioned, the noise sources for predicting tonal noise of rotating blade are computed by NVLM/VPM simulation. The time-series of aerodynamic loads acting on the surface of the rotor blades and their geometry information are used to calculate the acoustic pressure at given observer position in the time domain. Only acoustic data in the time domain after 15 revolutions, rather than overall time history across all revolutions, are utilized on the acquiring acoustic results in the frequency domain. This post-processing technique can help to more accurately capture the tonal acoustic amplitudes at principal frequencies of interests. Acoustic spectra at five observer positions are computed using the fast Fourier Transform (FFT) with a Hanning window function. After which, noise amplitudes of each frequency of interest are computed by calculating the RMS of the ensemble-averaged pressure time history as in Equation 4, where p_{ref} is 20 μPa .

$$SPL = 20 \log_{10} \left(\frac{\bar{P}_{rms}}{P_{ref}} \right) \quad \text{Eq. (4)}$$

Figure 4 presents the 1st BPF directivity of the isolated rotor for a range of rotor rotation rates including 4800, 5400, and 6000 rpm. Calculations are compared with experimental acoustic data and two predictions with different simulation techniques. OF2-PSW indicates the prediction results of a coupled analysis using high-fidelity OVERFLOW2 CFD and PSU-WOPWOP solvers, while ANOPP-PAS denotes the

simulation results of blade element analysis and Farassat's 1A formula. The comparison results show that the 1st BPF predictions in terms of acoustic amplitudes and directivity are well-matched with measurements. However, in the present work, acoustic analysis is limited to a tonal noise prediction at 1st BPF. Other harmonic noise at the principal rotor-associated frequencies and broadband noise cannot be clearly observed.

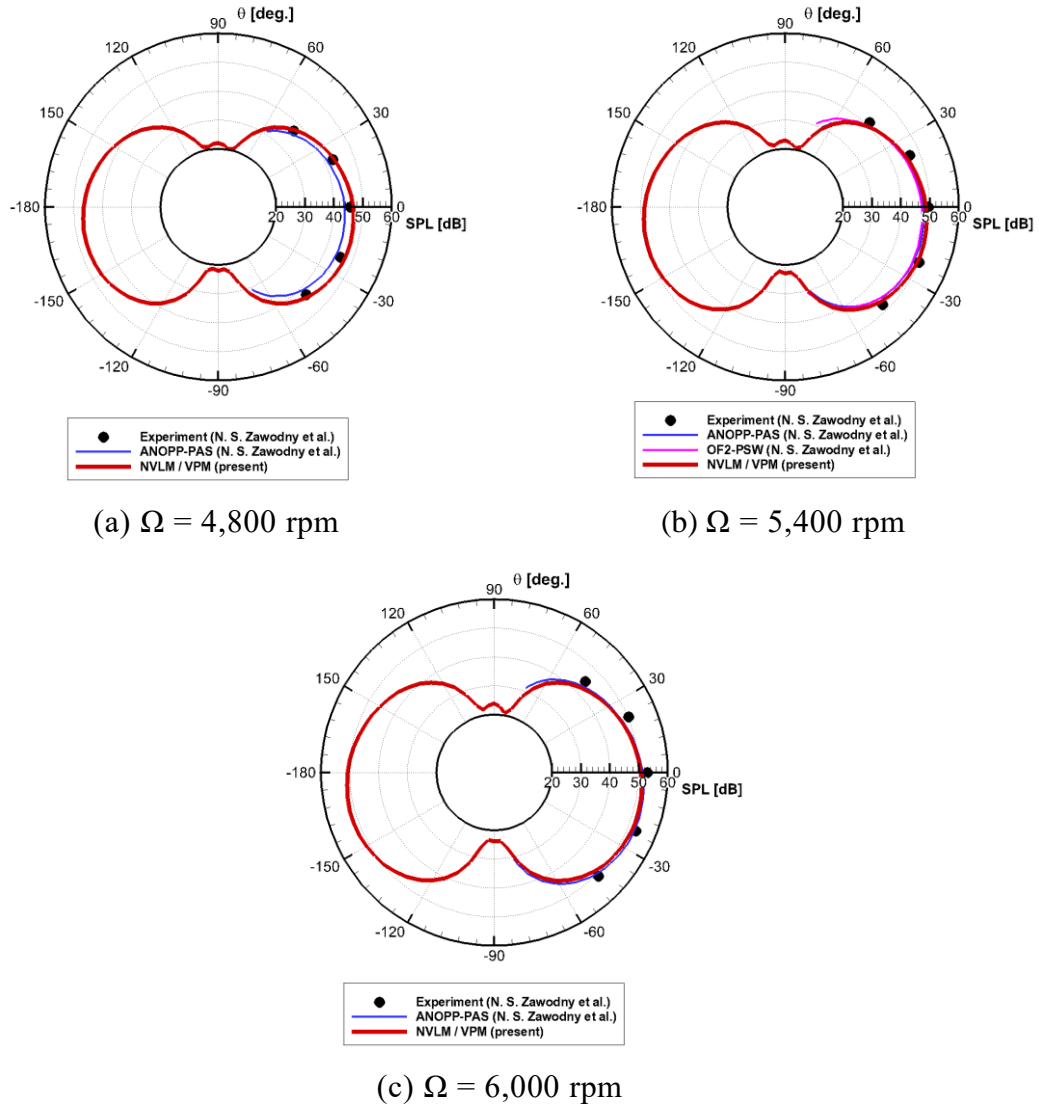


Figure 4. Comparison of 1st BPF directivity of isolated rotor depending on rotating speeds

3.2 Quadcopter configuration

Calculations for quadcopter configuration with different separation distance were performed to study the effects of the rotor-to-rotor interaction on noise characteristics of small-scale UAV. The separation distance (d) is defined as a length between neighboring rotor tips, and it is varied from $0.2D$ to $1.0D$. Here D is the rotor diameter. Numerical simulations of quadcopter were carried out at the rotational speed of 5,400 rpm.

Figure 5 shows the comparison of the OASPL (overall sound pressure level) directivity between isolated rotor and quadcopter configurations with different separation distances. It can be reasonably expected that resulting acoustic amplitudes of quadcopters significantly increase compared to those of isolated rotor as the noise sources including aerodynamic loading and the number of the rotor blades increase. Although an overall

agreement in terms of OASPL directivity trend is observed at quadcopter configurations with $d/D = 0.2$ and 1.0 , the sound pressure level of the quadcopter with $d/D = 0.2$ is much higher than that of the quadcopter with $d/D = 1.0$. It indicates that the separation distances between the rotors strongly affect the hover performance of quadcopter; As the separation distance between the rotor becomes smaller, a considerable thrust fluctuation occurs, even if the quadcopter UAV operates in hover flight condition. In addition, unsteady loading introduced by severe rotor interaction causes an increase in the sound pressure level, especially normal to the rotating plane ($\theta = 90^\circ$).

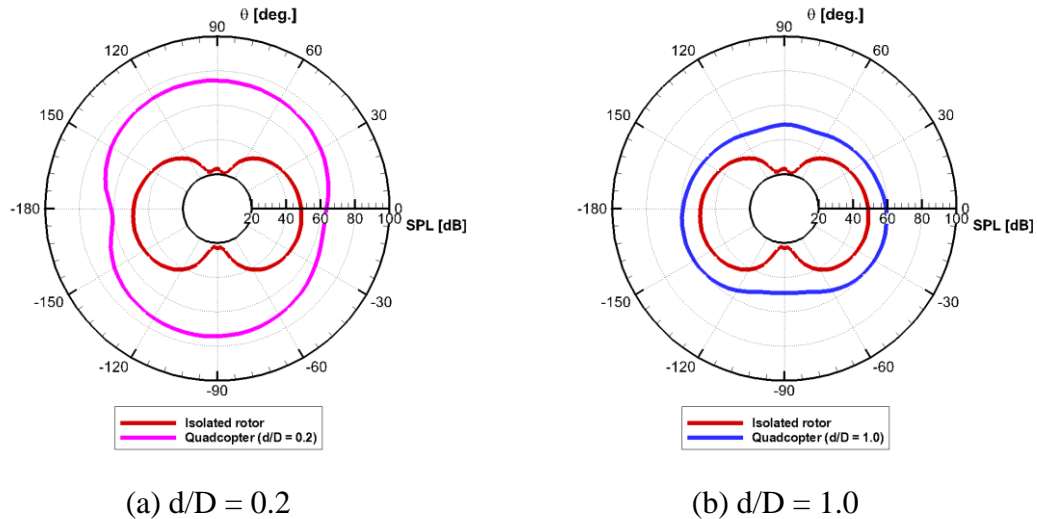


Figure 5. Comparison of OASPL directivity of quadcopter depending on separation distances

4. CONCLUSIONS

In the quadcopter configuration, the rotor interaction phenomenon severely occurs in the unmanned aerial vehicles (UAVs). Therefore, separation distance plays an important role in determining the aerodynamic performance and noise level of the UAVs with multi-rotor configuration. In this work, the computational study of a small size quadcopter UAV was carried out to investigate the rotor interaction effects on the acoustic characteristics. Calculations for quadcopter configuration showed that the sound pressure level of the quadcopter was much higher than that of the isolated rotor and a significant difference in noise directivity between the quadcopter and isolated rotor was clearly captured. It is found that unsteady loading introduced by rotor interaction leads to a considerable increase in noise level. This study is a preliminary study to the aeroacoustic problem in multicopter UAV. Discussion in this work gives scope for further research on noise reductions of multicopter UAV by controlling a separation distance between the rotors.

5. ACKNOWLEDGEMENTS

This research was supported by Development of Design Technologies for High Efficiency, Low Noise Propellers of Multi-copter UAVs through the National Research Foundation of Korea (NRF), funded by the Ministry of Science, ICT & Future Planning (No. 2016937799).

6. REFERENCES

1. N.S. Zawodny, D.D. Boyd Jr and C.L. Burley, "*Acoustic Characterization and Prediction of Representative, Small-Scale Rotary-Wing Unmanned Aircraft System Components*", American Helicopter Society (AHS) 72nd Annual Forum Proceedings, West Palm Beach, Florida, USA, May 17-19, 2016.
2. H. Lee and D.J. Lee, "*Numerical investigation of the aerodynamics and wake structures of horizontal axis wind turbines by using nonlinear vortex lattice method*", Renewable Energy, 132, pp. 1121-1133, 2019.
3. H. Lee and D.J. Lee, "*Wake impact on aerodynamic characteristics of horizontal axis wind turbine under yawed flow conditions*", Renewable Energy, 136, pp.383-392, 2019.
4. H. Lee and D.J. Lee, "*Computational study of wake interaction in quadcopter unmanned aerial vehicle*", 7th Asian/Australian Rotorcraft Forum (ARF) Proceedings, Jeju Island, Korea, Oct. 30-Nov. 1, 2018.
5. F. Farassat and G.P. Succi, "*The Prediction of Helicopter Rotor Discrete Frequency Noise*", Vertica, 7(4), pp. 309-320, 1983.